Front. Mater. Sci. 2024, 18(1): 240671
https://doi.org/10.1007/s11706-024-0671-2

RESEARCH ARTICLE

Bioactivity of silk fibroin peptides on vascular endothelial cells

Mengnan Dai*, Meng Li*, Peixuan Li, Boyu Zhang, Jianmei Xu, and Jiannan Wang (✉)

National Engineering Laboratory for Modern Silk, College of Textile and Clothing Engineering, Soochow University, No. 199 Ren-ai Road, Suzhou Industrial Park, Suzhou 215123, China

ABSTRACT: To determine the contribution of non-repetitive domains to the bioactivity of the heavy chain in silk fibroin (SF) macromolecules, a gene motif f(1) encoding this fragment and its multimers (f(4) and f(8)) were biosynthesized from *Escherichia coli* BL21. Based on the positive application potential of SF materials for the vascular tissue engineering, this study focused on examining the active response of these polypeptides to vascular endothelial cells. Biosynthetic polypeptides F(1), F(4), and F(8) were separately grafted onto the surfaces of bioinert polyethylene terephthalate (PET) films, resulting in remarkable improvements in the spread and proliferation of human umbilical vein endothelial cells (HUVECs). Using the same grafting dose, the activity of cells on polypeptide-modified PET films enhanced with the increase of the molecular weight of those grafted polypeptides from F(1) to F(8). Meanwhile, the growth of cells on the surface of the alkaline-treated PET film was improved, indicating that the hydrophilicity of the surface material had influence on the growth of HUVECs. Moreover, on surfaces with the same water contact angle, the spread and proliferation activity of cells on PET films were significantly lower than those on polypeptide-modified PET films.

KEYWORDS: silk fibroin heavy chain; non-repetitive fragment; cytoactive; endothelial cell

Contents

Received July 17, 2023; accepted November 21, 2023

E-mail: wangjn@suda.edu.cn

* M.D. and M.L. contributed equally to this work.

1 Introduction

A *Bombyx mori* silk fibroin (SF) macromolecule is composed of six heavy chains (H-chains), six light chains (L-chains), and one P25 glycoprotein chain [1]. The H-chain is the major component of a SF macromolecule, consisting of an N-terminal domain, a C-terminal domain, and a middle core area which is arranged alternately by 12 repetitive regions (mainly GAGAGS hexapeptide repeats) and 11 non-repetitive regions (SGFGPVANGG SGEASSESDFGSSGFGPVANASSGEASSESDFAG) [2]. Given the increased use of SFs in biomaterials research, we are interested in determining the functions of the corresponding H-chain in SFs on biological activity and in clarifying the sequences of its activity.

SF materials have been proven to possess satisfactory biocompatibility, such as anticoagulant activity and cell proliferative activity, which are widely acceptable to be used in the field of tissue engineering. In the three-dimensional (3D) porous scaffolds prepared with SFs, smooth muscle cells (SMCs) can proliferate, secrete extracellular matrix (ECM) components, and survive for a long time. The ability of SMCs to express ECM-related genes can be regulated by the transforming growth factor β1 (TGF-β1) [3], which has significant application value in the design and fabrication of active tissue engineering scaffolds. Moreover, SFs have different regulatory effects on the growth of endothelial cells (ECs) and SMCs [4]. It has been revealed that SF materials are preferred for the adhesion of vascular ECs. Therefore, SF-based small-diameter artificial blood vessels can induce rapid endothelialization within two weeks and promote autologous vascular tissue regeneration *in situ*, maintaining long-term patency [5]. Additionally, SFs can support and promote stem cell differentiation. The SF scaffolds with a low β-sheet content, the modulus of which is similar to that of native ECs, can induce the differentiation of bone marrow mesenchymal stem cells (MSCs) into ECs [6].

The excellent biological activities of SFs are contributed by functional sequences in the macromolecules. Yamada et al. reported that two segments, VITTDSDGNE and NINDFDED, in the N-terminal region of the H-chain could promote the growth activity of human fibroblasts [7]. GAGAGS, GAGAGA, and GAGAGY, highly repetitive sequences derived from the core domain of the H-chain, were reported to be capable of promoting the proliferation of 3T3-L1 cells [8]. As an important tool for studying proteomics, in recent years, the genetic engineering technology has been extensively used to design and biosynthesize fragments derived from silk, spider silk, and collagen. A silk-elastin-like polypeptide recombining SF motif (GAGAGS) and mammalian elastin motif (VPAVG) was expressed by *Escherichia coli*, which could slightly enhance the cell viability of mouse myoblasts [9]. A fusion protein recombining a repetitive sequence $(GAGAGS)_n$ from the *Bombyx mori* SF and a collagen-like domain from the *S. pyogenes* bacterial collagen was expressed by *Escherichia coli* BL21 for studying the cell activity. This fusion protein could promote the proliferation and differentiation of human bone marrow MSCs [10].

However, the bioactivity of highly conserved non-repetitive sequences in the core domain of the H-chain has not been studied yet. As SF materials or composites have been increasingly studied for the application in vascular tissue engineering materials [11–13], it is extremely important to investigate the effect of those polypeptides on the activity of vascular cells, particularly of vascular ECs. In our previous work, a gene motif f(1) encoding a non-repetitive polypeptide of the H-chain was designed, cloned, and multimerized four times (f(4)) and eight times (f(8)) by the genetic engineering technique. The expression products were successfully synthesized in *Escherichia coli* BL21 [2,14], which were named as F(1), F(4), and F(8), respectively. Based on the application potential of SFs for the vascular tissue engineering, in this work, we focused on studying the bioactivities of polypeptides F(1), F(4), and F(8) on human umbilical vein endothelial cells (HUVECs). Specifically, polypeptides were grafted onto the surfaces of bioinert polyethylene terephthalate (PET) films, and the effect of polypeptides on cell adhesion and cell proliferative activity was investigated following the seeding of HUVECs.

2 Materials and methods

2.1 Protein expression

Expression vectors pGEX-f(1), pGEX-f(4), and pGEX-f(8) which respectively carried a gene motif f(1), encoding the non-repetitive sequence derived from the H-chain, and its multimers f(4) (with four copies) and f(8) (with eight copies) were constructed as previously reported [2]. The expression vectors were separately transformed into

Escherichia coli BL21 cells and cultured in the Luria–Bertani (LB) solid medium to express the glutathione-S-transferase (GST)-tagged fusion proteins GST-F(1), GST-F(4), and GST-F(8) [14]. After the induction of isopropyl-β-D-thiogalactopyranoside (IPTG), cells were harvested by centrifugation at 4 °C and then stored at −80 °C prior to the protein purification.

2.2 Purification of target polypeptides

Fusion proteins were purified by a GST affinity purification system (Novagen, Billerica, MA, USA), as previously described [15]. Briefly, the cell pellet was suspended in the GST-binding buffer and sonicated on ice. Subsequently the lysate was centrifuged at 4 °C, and the supernatant was loaded onto a GST affinity column and washed with the GST-washing buffer. The GST-tagged fusion protein was then eluted with the GST-elution buffer containing reduced glutathione, followed by the loading onto a Sephadex G-15 gel (Solarbio, Beijing, China) to remove glutathione and salt. Afterwards, the purified fusion protein was digested with thrombin (Novagen) at 20 °C for 16 h, and the reaction mixture was loaded onto the GST affinity column again to remove the GST-tag, thus obtaining the polypeptides F(1), F(4), and F(8) that underwent a freeze-drying process finally.

2.3 Grafting of polypeptides onto PET films

PET films were cut and placed at the bottom of 24-well tissue culture plates 15.6 mm in diameter, and the surfaces of PET films were hydrolyzed with 0.5 mol·L^{-1} NaOH at 95 °C for 90 min. Following washing and air-drying, the hydrolyzed PET film (hereafter designated as PET-H1) was activated by 1 mg·mL^{-1} 1-ethyl-3-(3-dimethylamino-propyl) carbodiimide at 37 °C for 60 min, and the polypeptides, i.e., F(1), F(4), and F(8), with 2 mg·mL^{-1} N-hydroxysuccinimide and 0.05 mol·L^{-1} 2-(N-morpholino)ethanesulfonic acid (MES) were subsequently added. After reaction overnight at 4 °C, the produced mixtures were removed, followed by the washing of films for three times with phosphate-buffered saline (PBS; pH 7.4).

2.4 Coomassie brilliant blue staining

Coomassie brilliant blue (CBB) staining was used to directly observe the contents and distributions of polypeptides grafted onto the PET surfaces. As previously reported [16], the CBB staining solution was separately added onto the polypeptide-modified PET films, the hydrolyzed PET films, and the untreated PET film. Then films were incubated at room temperature for 1 h, followed by removal of the background color with the destaining solution. At last, the semi-quantitative analysis on PET films stained by CBB was performed by Image J 2.1.0 software.

2.5 Surface element assay

Surface chemical compositions of all PET films were analyzed by X-ray photoelectron spectroscopy (XPS) with an Axis Ultra HAS X-ray photoelectron spectrometer (Kratos Analytical Ltd., Manchester, UK) equipped with the Al Kα radiation source, and all binding energies were referenced to the C 1s peak of the surface adventitious carbon at 284.8 eV. Besides, the quantitative analysis of elements was performed by the XPS peak fitting program XPSPEAK version 4.1 [17].

2.6 Surface water contact angle measurement

The surface hydrophilicity of all the PET films was determined by the static water contact angle measurement. At first, a water droplet (5 μL) was placed on the surface of each film for 10 s, and all the contact angles were recorded on an OCA-50 contact angle goniometer (Dataphysics Inc., Germany). For each film, three replicate samples were analyzed. In addition, a film designated as PET-H2 with the water contact angle of 38° was prepared by further adjusting the water contact angle corresponding to the PET-H1 film (54°), ensuring that it was similar to those corresponding to polypeptide-grafted PET films.

2.7 Cell morphology and proliferation assay

HUVECs (ATCC, Manassas, VA, USA) were routinely cultured in Dulbecco's modified Eagle's medium (DMEM; Gibco, Carlsbad, CA, USA) supplemented with 10% (v/v) fetal bovine serum (FBS; Gibco, Carlsbad, CA, USA) and 1% (v/v) antibiotics (100 U·mL^{-1} penicillin and 100 μg·mL^{-1} streptomycin), followed by the growth at 37 °C in a humidified atmosphere containing 5% CO_2. When HUVECs reached a confluence level of 80%–90%, the cells were detached with 0.25% trypsin (Sigma, St. Louis, MO, USA) and resuspended at a density of 2.5×10^4 cells·mL^{-1}. Afterwards, a 1-mL aliquot of the HUVEC suspension (2.5×10^4 cells) was seeded into each

well pre-coated with the F(1)-, F(4)- or F(8)-modified PET film, followed by the incubation in a humidified atmosphere containing 5% CO_2 at 37 °C. After culturing for 1, 3, and 7 d, the cell morphology was separately observed by a TH4-200 inverted microscope. In addition, after culturing for 1, 3, 5, and 7 d, the proliferation of cells on different films was also evaluated separately by the Cell Counting Kit-8 (CCK-8) assay. At different culture time points, the culture medium was removed, and 400 μL of the cell culture medium mixed with 40 μL of the CCK-8 solution was directly added into each well. Subsequently, the cells were incubated for another 2 h, and eventually the optical density (OD) of the mixed medium was evaluated with a microplate reader at the wavelength of 450 nm. The PET film, hydrolyzed PET film, and tissue culture plate (TCP) without samples were used as controls, and all assays were performed in triplicate.

2.8 Statistical analysis

Statistical results were presented as the mean ± standard deviation (SD). The comparison of means was performed by the one-way analysis of variance (ANOVA), followed by independent Student's *t*-tests using the SPSS 17.0 statistical software (IBM, Armonk, NY, USA). Differences of $p < 0.05$ were considered statistically significant.

3 Results and discussion

3.1 Grafting ability and distribution of polypeptides on PET films

PET materials, such as vascular stents [18] and artificial blood vessels [19], have been widely used in clinical implantation surgeries, while they are biologically inert and not preferred for the adhesion and growth of various cells [20–21]. Hence, PET films were used as substrate materials, and polypeptides were grafted onto the film surfaces to subsequently evaluate the bioactivity of polypeptides on vascular cells. Figure 1(a) shows the distributions of polypeptides on the surfaces of PET films. It was observed that all the three polypeptides, F(1), F(4), and F(8), were successfully grafted, which were clearly

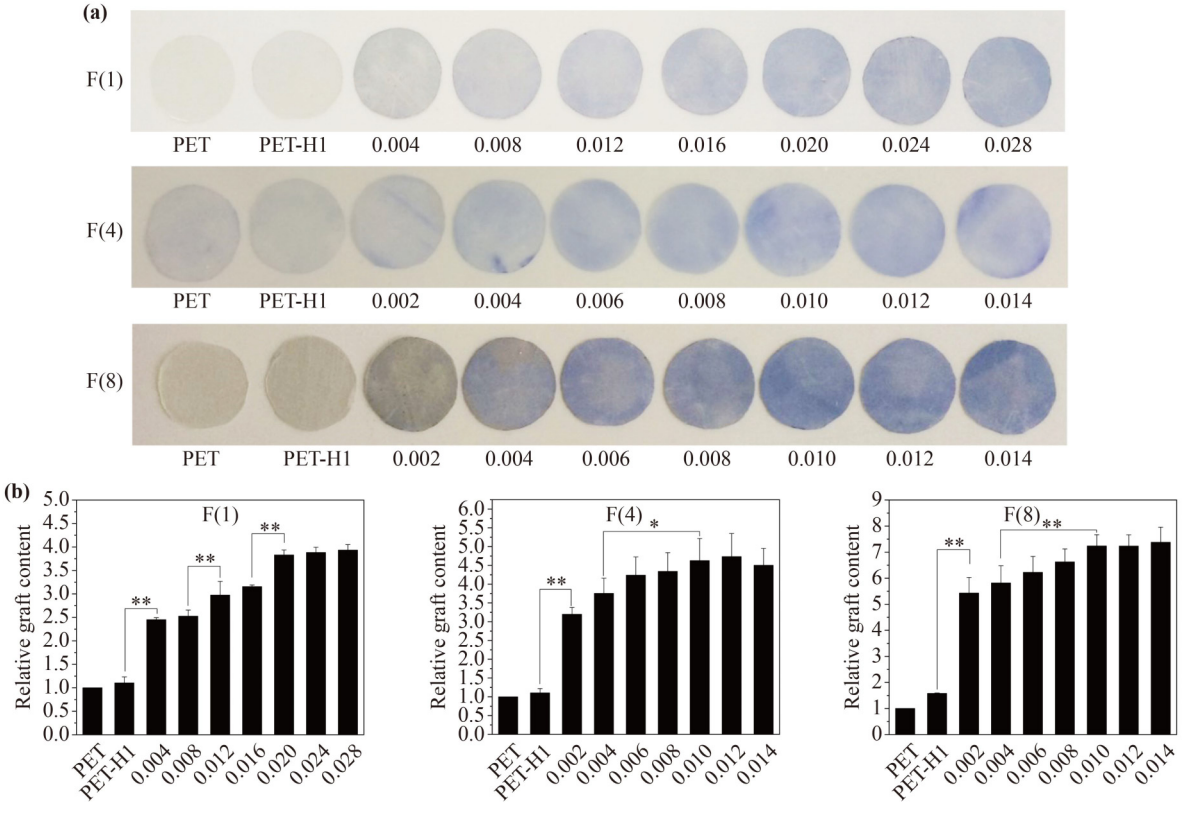

Fig. 1 CBB staining of the PET film surfaces after hydrolysis and grafting polypeptides with different graft reaction doses (μmol/well): (**a**) digital photographs; (**b**) semi-quantitative analysis. The relative values refer to the ratio to PET with $*p < 0.05$ and $**p < 0.01$.

visible after CBB staining. The color was evenly distributed on the film surface and gradually became darker with the increased amount of polypeptides. However, the color was not visible on the pristine and hydrolyzed PET films after CBB staining. When the molar concentration of the polypeptides added to the reaction was the same (such as 0.008 μmol/well), the blue color on the film surface deepened with the increase of the polypeptide molecular weight. Moreover, the color on polypeptide-modified PET films did not change visibly when the graft reaction doses of F(1), F(4), and F(8) were more than 0.02, 0.01, and 0.01 μmol/well, respectively, which were consistent with the semi-quantitative results (Fig. 1(b)).

3.2 Surface chemical structure of polypeptide-modified PET films

The PET macromolecule consists of three elements C, H, and O, and the main chain mainly includes benzene rings, ester groups, and methylenes. Following the sodium hydroxide treatment, ester groups on the film surface were hydrolyzed to release −COOH and −OH. As shown in Fig. 2, two separate peaks corresponding to C 1s (286 eV) and O 1s (532 eV) were observed as the main elements in the PET film (Fig. 2(a)) and the hydrolyzed PET film (Fig. 2(b)), and the O 1s characteristic peak of the hydrolyzed PET film was significantly enhanced due to the hydrolysis of ester groups on the surface. The XPS spectra showed that a clear N 1s peak at the binding energy of 400 eV appeared after the polypeptides F(1), F(4), and F(8) were grafted, indicating the stable grafting of polypeptides onto the PET film surface (Figs. 2(c)–2(e)). The peak intensity was enhanced with the growth of the peptide chain from F(1) to F(8), indicating that the content of the N element on the film surface increased. These results were consistent with the CBB staining results.

Further split-peak fitting data of N 1s in Table 1 showed that the content of C−N/N−C=O increased as the molecular weight of grafted polypeptides rose from F(1) to F(8), while the content of N−H decreased, which was due to $-NH_2$ in polypeptides interacting with −COOH on the surface of the PET film, gradually increasing the amount of N−C=O generated. The split-peak fitting of O 1s revealed that O−H in the hydrolyzed PET increased significantly due to the hydrolysis of ester bonds. As the longer polypeptide segment contains more −OH, the content of O−H on PET films grafted with polypeptide segments increased from F(1) to F(8).

3.3 Surface wettability of polypeptide-modified PET films

PET materials have poor hydrophilicity as the macromolecular chain has no hydrophilic groups except

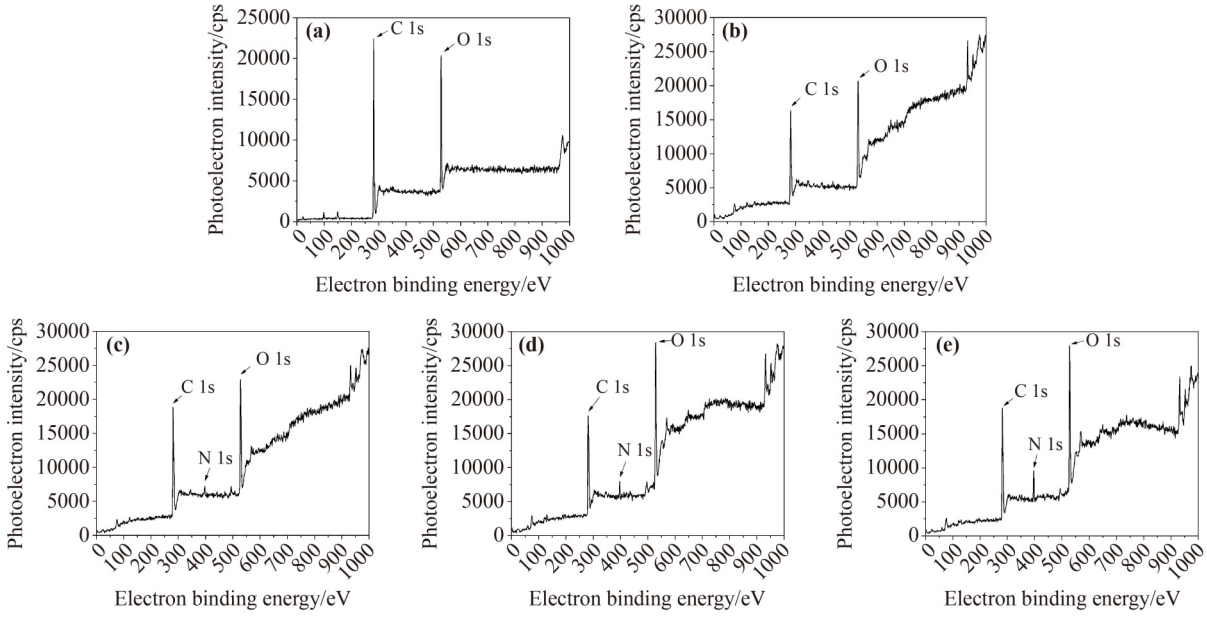

Fig. 2 XPS energy spectra of the PET film surfaces: (**a**) PET film; (**b**) PET-H1 film; (**c**) F(1)-modified PET film; (**d**) F(4)-modified PET film; (**e**) F(8)-modified PET film. The graft reaction doses for all three polypeptides are 0.008 μmol/well.

Table 1 Elements and chemical states on the surfaces of several films

Sample	Element content/%		Area fraction of each chemical state after O 1s and N 1s peak fitting/%			
	O	N	O 1s		N 1s	
			O=C−O/N−C=O	O−H	C−N/N−C=O	N−H
PET	45.86	0	66.62	33.38	0	0
PET-H1	51.43	0	60.90	39.10	0	0
F(1)	51.56	2.60	59.50	40.50	47.35	73.51
F(4)	51.56	5.76	58.35	41.65	51.74	48.26
F(8)	46.56	10.20	52.65	47.35	71.60	24.40

for the two −OH groups at the end. After hydrolysis, the surface wettability of the PET-H1 film was improved with the change of the static water contact angle from 77° to 54°. When the surface of the PET film was modified with polypeptides, the static water contact angle decreased significantly and was graft-dependent, as shown in Fig. 3. These polypeptide chains contained more hydrophilic amino acids, such as glutamic acid, aspartic acid, and serine in F(1), F(4), and F(8), which improved the surface wettability of PET films.

3.4 Cell affinity on polypeptide-modified PET films

To assess the biological activity of the three polypeptides, HUVECs were seeded onto the surfaces of polypeptide-modified PET films, and the numbers of viable growing cells were investigated after culturing for 1, 3, and 7 d. The cell morphologies of HUVECs cultured on the PET film and polypeptide-modified PET films are shown in Fig. 4(a). HUVECs underwent better spreading into spindle, triangular, or polygonal shapes on polypeptide-modified PET films compared with PET and hydrolyzed PET films after seeding for 24 h. Many cells began to emerge at the 3rd day while fully covered the surfaces at the 7th day after seeding on the polypeptide-modified PET films, and it is observed that cells on the PET film and the polypeptide-modified PET films had great differences in both morphology and number. Figure 4(b) shows the cell proliferation viability by quantitative analysis. The HUVECs proliferation activity on PET films was significantly improved after the grafting of polypeptides, and was further enhanced by the addition of grafted

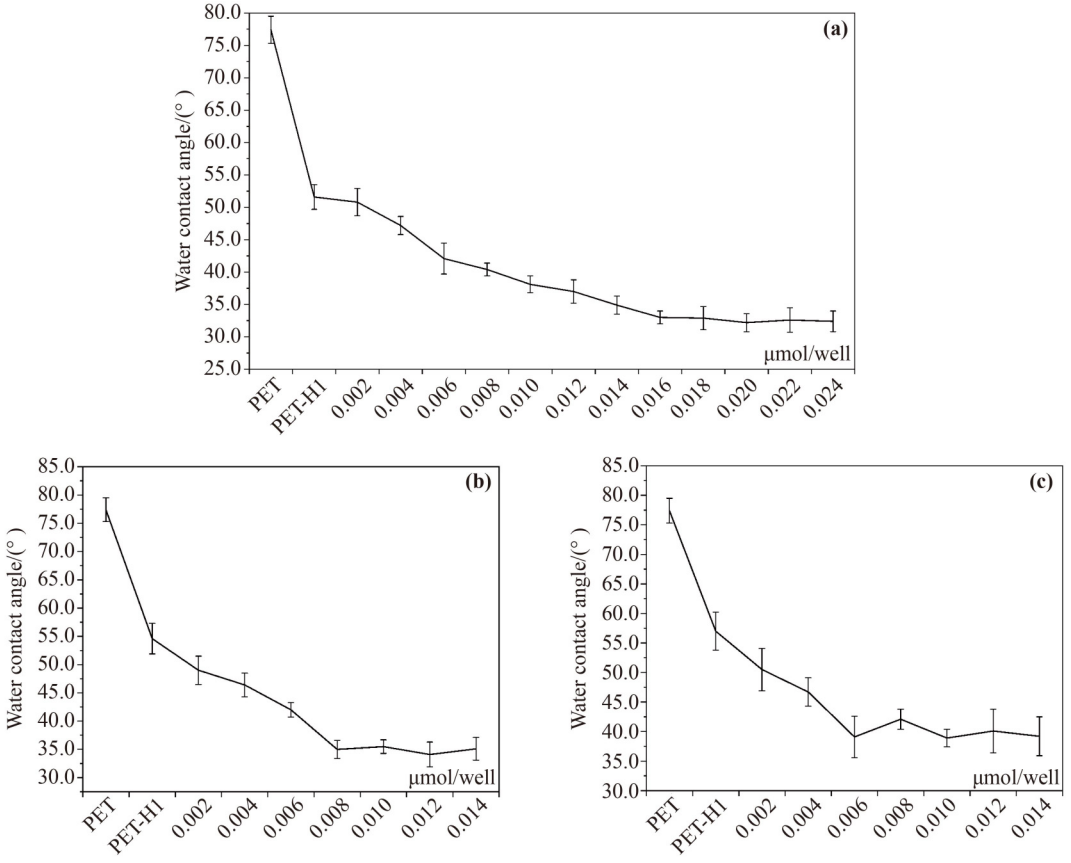

Fig. 3 Changes of water contact angles for the PET films after hydrolysis and grafting polypeptides: (**a**) F(1)-modified PET film; (**b**) F(4)-modified PET film; (**c**) F(8)-modified PET film.

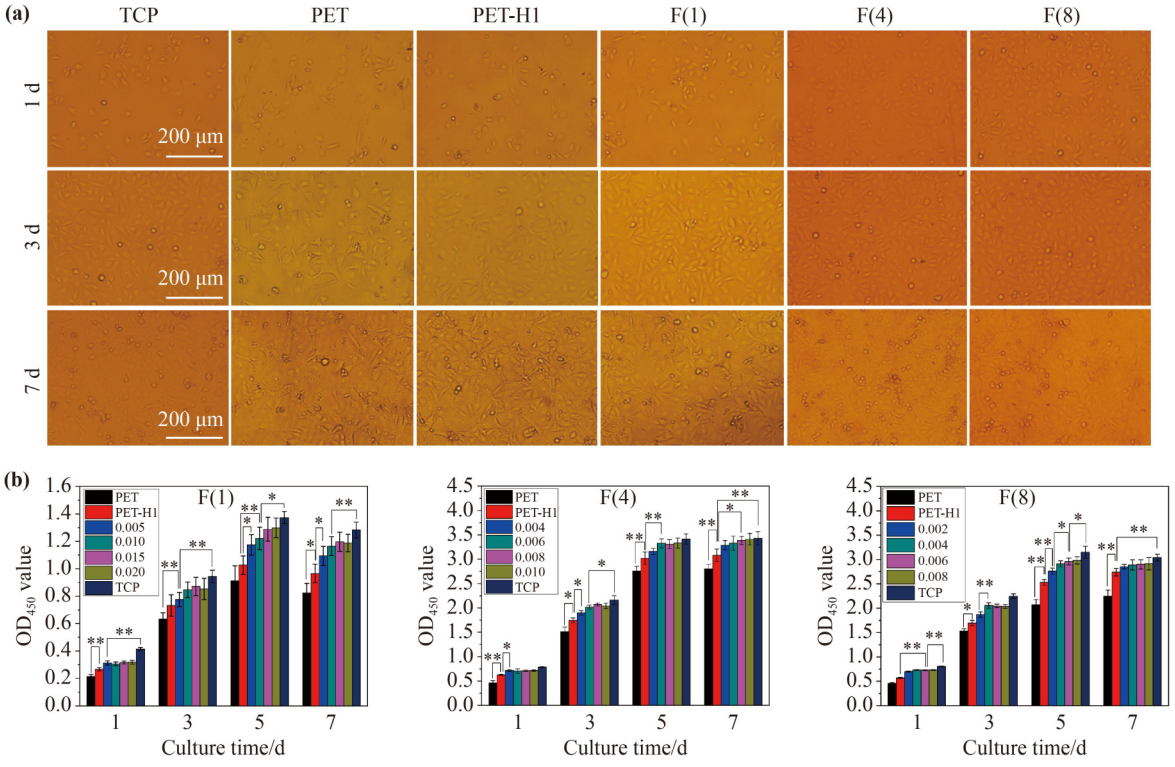

Fig. 4 The growth of cells on polypeptide-modified PET films: (**a**) cell morphologies (the graft reaction doses are 0.01 μmol/well for F(1), 0.01 μmol/well for F(4), and 0.008 μmol/well for F(8)); (**b**) cell viabilities on polypeptide-modified PET films (*$p < 0.05$ and **$p < 0.01$). TCP, PET, and PET-H1 films are used as controls.

polypeptides. When the graft reaction doses of F(1), F(4), and F(8) were 0.015, 0.006, and 0.004 μmol/well, respectively, the proliferation activities of cells on the surfaces of those modified films reached the highest. The number of adherent cells gradually rose with the increase of the incubation time up to 5 d, and as the incubation time was prolonged to 7 d, the percentage of proliferating cells reached a constant value and even began to slightly decrease, as there was no more space for cell proliferation, which might result in cell apoptosis.

Figure 5 shows the relative proliferation rates of HUVECs on the surfaces of all films. The relative proliferation rate of HUVECs on the hydrolyzed PET film was significantly larger than that on the PET film. This may be attributed to the increased hydrophilicity of the film surface and the release of carboxyl groups on the surface, promoting cell adhesion and proliferation [22]. The relative proliferation rates of HUVECs on polypeptide-modified PET films were significantly larger than that on the hydrolyzed PET film, as well as increasing with the addition of grafted polypeptides. These findings showed that polypeptide-modified PET films markedly enhanced the rate of division and proliferation of HUVECs, especially when the cells were in the logarithmic growth phase. The results also showed that the relative proliferation rate of the F(4)-modified PET film (117%) was a little larger than that of the F(1)-modified one (115%) when both of their corresponding graft reaction doses were 0.01 μmol/well, while the relative proliferation rate of the F(8)-modified PET film (121%) was obviously larger than that of the F(4)-modified one (108%) corresponding to the identical graft reaction doses of 0.004 μmol/well. These results might be attributed to both the larger molecular weight and the larger surface modification area of the peptide chain in contact with the PET film.

In addition, it was found that the surface of the hydrolyzed PET film also promoted the proliferation activity of HUVECs. Studies indicated that, compared with the hydrophobic surface, the hydrophilic surface was more conducive to cell adhesion and proliferation [23] as well as endothelialization of vascular grafts [24]. As the surface hydrophilicity of polypeptide-modified PET films was further improved compared with that of the hydrolyzed PET film, in order to exclude the effect of hydrophilicity on cells and accurately analyze the

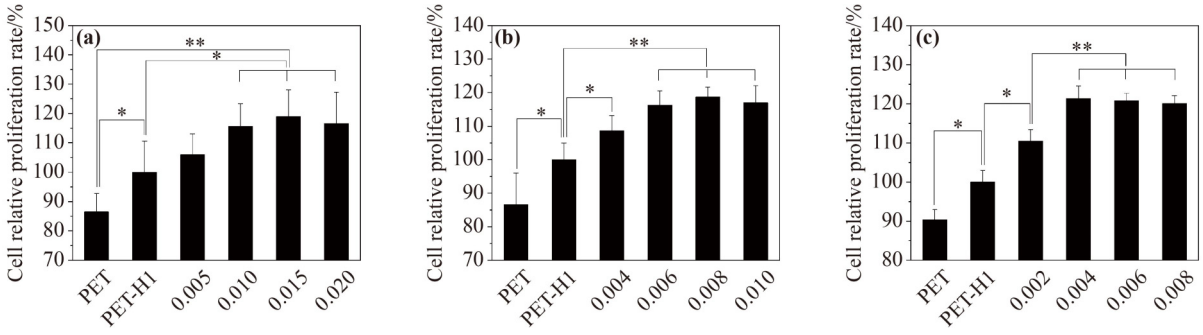

Fig. 5 Cell relative proliferation rates of HUVECs at the 3rd day on polypeptide-modified PET films with different graft reaction doses (μmol/well): (**a**) F(1)-, (**b**) F(4)-, and (**c**) F(8)-modified PET films relative to that on the PET-H1 film (*$p < 0.05$ and **$p < 0.01$). PET and PET-H1 films are used as controls.

biological activity of polypeptides, we further studied the growth behaviors of HUVECs on several films with similar water contact angles, including hydrolyzed PET films and polypeptide-modified PET films. At first, a hydrolyzed PET film with the surface water contact angle of 38° was obtained by adjusting the hydrolysis reaction. When the graft reaction doses of F(1), F(4), and F(8) reached 0.02, 0.008, and 0.006 μmol/well, the water contact angles were 32°, 35°, and 39°, respectively (Table 2). As shown in Figs. 6(a) and 6(b), the numbers of HUVECs on F(1)-, F(4)-, and F(8)-modified PET films were significantly larger than the numbers of those on the PET film and two types of hydrolyzed PET films. Moreover, the water contact angle of the F(8)-modified PET film (39°) was larger than those of the F(1)-modified film (32°) and the F(4)-modified film (35°), while the cell proliferation activities were almost the same for above-mentioned three polypeptide-modified PET films but significantly higher than that for the PET-H2 film with a similar water contact angle (38°) revealed by Figs. 6(c)–6(e). As for the two types of hydrolyzed PET films, it was detected that the proliferation activity of HUVECs on the surface of the PET-H2 film with the water contact angle of 38° was slightly higher than that of the PET-H1 film with the water contact angle of 54°, while their difference was little.

According to the further analysis on the relative cell proliferation activity (Figs. 6(c)–6(e)), the relative cell proliferation rates of HUVECs on polypeptide-modified PET films were much larger than that on the PET-H2 film, despite the fact that their water contact angles were almost identical, indicating that the polypeptides effectively enhanced the proliferation ability of HUVECs. During the logarithmic growth phase, the relative proliferation rate of HUVECs on the F(8)-modified PET film was larger than those on F(1)- and F(4)-modified PET films, whereas their difference was little.

Table 2 Several films with similar water contact angles

Sample	Water contact angle/(°)
F(1)-modified PET film	32
F(4)-modified PET film	35
F(8)-modified PET film	39
PET-H2 film	38
PET-H1 film	54
PET film	77

4 Conclusions

F(1), a structural component of the non-repetitive domain of the H-chain in SFs, and the repeats F(4) and F(8) were stably and efficiently expressed using the genetic engineering technology. The target polypeptides F(1), F(4), and F(8) were stably and uniformly grafted onto the surfaces of bioinert PET films, which was verified by CBB staining. With the same graft reaction dose, the greater the molecular weight of the polypeptide, the darker the stain color. The hydrophilicity of the PET surface was significantly improved after grafting with polypeptides, so was the proliferation activity of cells on the PET surface. At the same graft reaction dose, the cell proliferation ability increased with increasing polypeptide chains from F(1) to F(8). The surface water contact angle of the PET film grafted with F(8) was slightly larger than those with F(1) and F(4), while there was no significant difference in the proliferation activity of cells on such three polypeptide-grafted PET films. As for two types of hydrolyzed PET films, although there was obvious difference in water contact angles, the proliferation

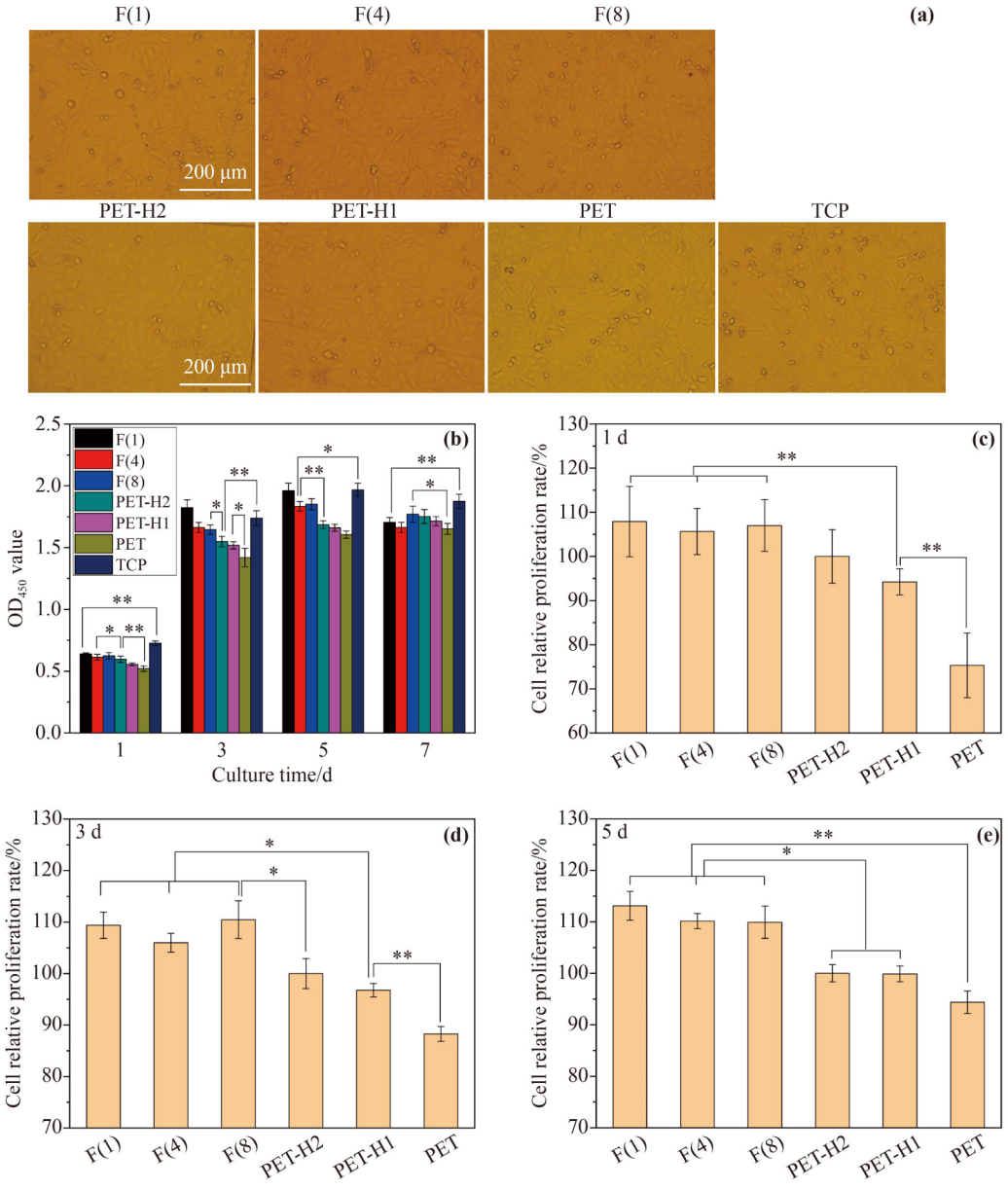

Fig. 6 Cells growth on the films with similar water contact angles: (**a**) cell morphologies at the 5th day; (**b**) cell viabilities; (**c**)(**d**)(**e**) proliferation rates of cells on PET, PET-H1, and polypeptide-modified PET films relative to that on the PET-H2 film. The graft reaction doses are 0.02 μmol/well for F(1), 0.008 μmol/well for F(4), and 0.006 μmol/well for F(8), with $*p < 0.05$ and $**p < 0.01$.

activities of cells on the surfaces of such two films were similar. The surface water contact angle of the PET film grafted with F(8) was similar to that of the hydrolyzed PET-H2 film. However, the cell proliferation activity corresponding to the former was significantly higher than that corresponding to the latter, showing that those three polypeptides had significant pro-proliferation activity on HUVECs when the factor of surface hydrophilicity was eliminated. This work reveals that the non-repetitive domain of the H-chain in SFs has clear potential in vascular tissue engineering applications.

Disclosure of competing interests The authors declare that they have no known competing financial interests or personal relationships that could have appeared to influence the work reported in this paper.

Acknowledgements This work was supported by the National Natural Science Foundation of China (Grant No. 51873141). We thank International Science Editing for editing this manuscript.

References

[1] Xu J J, Wang Y N, Ding M Y, et al. Sequence-structure characterization of recombinant polypeptides derived from silk

fibroin heavy chain. Materials Science and Engineering C, 2020, 111: 110831

[2] Huang H Y, Tian Z F, Yi H G, et al. Designing and cloning of the gene sequence encoding silk fibroin amorphous domain. Journal of Donghua University (English Edition), 2012, 29(6): 489–492

[3] Song G Z, Zheng C D, Liu Y F, et al. In vitro extracellular matrix deposition by vascular smooth muscle cells grown in fibroin scaffolds, and the regulation of TGF-β1. Materials & Design, 2021, 199: 109428

[4] Alessandrino A, Chiarini A, Biagiotti M, et al. Three-layered silk fibroin tubular scaffold for the repair and regeneration of small caliber blood vessels: from design to *in vivo* pilot tests. Frontiers in Bioengineering and Biotechnology, 2019, 7: 356

[5] Li H L, Wang Y N, Sun X L, et al. Steady-state behavior and endothelialization of a silk-based small-caliber scaffold in vivo transplantation. Polymers, 2019, 11(8): 1303

[6] Bai S M, Han H Y, Huang X W, et al. Silk scaffolds with tunable mechanical capability for cell differentiation. Acta Biomaterialia, 2015, 20: 22–31

[7] Yamada H, Igarashi Y, Takasu Y, et al. Identification of fibroin-derived peptides enhancing the proliferation of cultured human skin fibroblasts. Biomaterials, 2004, 25(3): 467–472

[8] Kim E D, Bayaraa T, Shin E J, et al. Fibroin-derived peptides stimulate glucose transport in normal and insulin-resistant 3T3-L1 adipocytes. Biological & Pharmaceutical Bulletin, 2009, 32(3): 427–433

[9] Machado R, Azevedo-Silva J, Correia C, et al. High level expression and facile purification of recombinant silk-elastin-like polymers in auto induction shake flask cultures. AMB Express, 2013, 3(1): 11

[10] An B, DesRochers T M, Qin G, et al. The influence of specific binding of collagen–silk chimeras to silk biomaterials on hMSC behavior. Biomaterials, 2013, 34(2): 402–412

[11] Kuang H Z, Wang Y, Shi Y, et al. Construction and performance evaluation of Hep/silk–PLCL composite nanofiber small-caliber artificial blood vessel graft. Biomaterials, 2020, 259: 120288

[12] Li H L, Song G Z, Tian W, et al. Motility and function of smooth muscle cells in a silk small-caliber tubular scaffold after replacement of rabbit common carotid artery. Materials Science and Engineering C, 2020, 114: 110977

[13] Xu S, Li Q T, Pan H T, et al. Tubular silk fibroin/gelatin-tyramine hydrogel with controllable layer structure and its potential application for tissue engineering. ACS Biomaterials Science & Engineering, 2020, 6(12): 6896–6905

[14] Yang G Q, Wu M Y, Yi H G, et al. Biosynthesis and characterization of a non-repetitive polypeptide derived from silk fibroin heavy chain. Materials Science and Engineering C, 2016, 59: 278–285

[15] Zhao H R, Yang Y X, Yi H G, et al. Biosynthesis of a potentially functional polypeptide derived from silk fibroin. Bio-Medical Materials and Engineering, 2014, 24(6): 2057–2064

[16] Wang J N, Yan S Q, Lu C D, et al. Biosynthesis and characterization of typical fibroin crystalline polypeptides of silkworm *Bombyx mori*. Materials Science and Engineering C, 2009, 29(4): 1321–1325

[17] Shi P G, Zhang L, Tian W, et al. Preparation and anticoagulant activity of functionalised silk fibroin. Chemical Engineering Science, 2019, 199: 240–248

[18] Jaziri H, Mokhtar S, Kyosev Y, et al. Influence of fatigue stress on the radial strength of polymeric braided vascular stents. Polymers for Advanced Technologies, 2022, 33(2): 627–637

[19] Jirofti N, Mohebbi-Kalhori D, Samimi A, et al. Fabrication and characterization of a novel compliant small-diameter PET/PU/PCL triad-hybrid vascular graft. Biomedical Materials, 2020, 15(5): 055004

[20] Van de Voorde B, Benmeridja L, Giol E D, et al. Potential of poly(alkylene terephthalate)s to control endothelial cell adhesion and viability. Materials Science and Engineering C, 2021, 129: 112378

[21] Giol E D, Van Vlierberghe S, Unger R E, et al. Biomimetic strategy towards gelatin coatings on PET. Effect of protocol on coating stability and cell-interactive properties. Journal of Materials Chemistry B: Materials for Biology and Medicine, 2019, 7(8): 1258–1269

[22] Tzoneva R, Seifert B, Albrecht W, et al. Poly(ether imide) membranes: studies on the effect of surface modification and protein pre-adsorption on endothelial cell adhesion, growth and function. Journal of Biomaterials Science: Polymer Edition, 2008, 19(7): 837–852

[23] Huang Z S, Bi L, Zhang Z Y, et al. Effects of dimethylolpropionic acid modification on the characteristics of polyethylene terephthalate fibers. Molecular Medicine Reports, 2012, 6(4): 709–715

[24] Jiang Y C, Wang H A, Wang X F, et al. Surface modification with hydrophilic and heparin-loaded coating for endothelialization and anticoagulation promotion of vascular scaffold. International Journal of Biological Macromolecules, 2022, 219: 1146–1154